

Synthesis of PbTiO₃ Thin Films by Annealing Multilayer Oxide Structures in Vacuum

A. ILJINAS^{a,*}, V. STANKUS^a AND R. KALIASAS^b

^aDepartment of Physics, Kaunas University of Technology, Studentų 50, LT-51368, Kaunas, Lithuania

^bDepartment of Technology, Kaunas University of Technology, Nemuno 33, LT-37164 Panevėžys, Lithuania

(Received January 25, 2015; in final form September 30, 2015)

This article presents investigation of syntheses of perovskite PbTiO₃ thin films by using reactive magnetron layer-by-layer deposition on Si (100) substrate and post-annealing in air and vacuum ($p = 5 \times 10^{-3}$ Pa). The film stoichiometry was accurately controlled by the deposition of individual layers with the required (≈ 1 nm) thickness, using the substrate periodic moving over targets. Deposited thin films were annealed in air and in vacuum at 670 °C and 770 °C for 1 h, respectively. The morphological, structural, and chemical properties of thin films deposited at 300 °C substrate temperature and post-annealed thin films using either conventional annealing and thermal annealing in vacuum at different temperatures were investigated and compared between. X-ray diffraction measurements of thin films annealed in air show formed crystalline perovskite PbTiO₃ phase with tetragonality $c/a = 1.047$. The crystallite size of oxidized films depends on the substrate temperature. The structure of post annealed in vacuum thin films strongly depends on Pb/Ti atomic ratio. It was observed that the best structure and morphology forms when atomic ratio of Pb/Ti was 0.80. Pseudocubic phase of lead titanate forms with sufficiently low tetragonality at 670 °C temperature.

DOI: [10.12693/APhysPolA.129.121](https://doi.org/10.12693/APhysPolA.129.121)

PACS/topics: 81.15.Cd, 68.55.-a

1. Introduction

Lead titanate is investigated until nowadays although the first report about lead titanate (PbTiO₃) was made by Shirane et al. in 1950 [1] due to its unique ferroelectric, pyroelectric, piezoelectric and other properties. PbTiO₃ and its solid solutions, as: PbTi_xZr_{1-x}O₃, (1-x)PbTiO₃-xBi(Ni_{1/2}Ti_{1/2})O₃ [2], Bi(Mg_{1/2}Zr_{1/2})O₃-PbTiO₃ [3], and other thin films have a great attention and perspective in application in electronic devices, such as: capacitors [4], ultrasonic transducers [5], thermistors [6], pyroelectric infrared detector [7, 8], optoelectronics [9], nonvolatile low voltage, and high speed memories (FRAM) [10, 11]. PbTiO₃ also exhibits the giant electrocaloric effect [12]. Lead titanate films, as other ferroelectric films were synthesized by various physical and chemical deposition methods. Many fabrication methods do not solve the problem of thin film density, well ordered crystal structure, and stoichiometry of films. Many fabrication methods report about lead loss [13], cracks in microstructure [14], stoichiometry problems [15], and non-uniformity of film surface using solid state reactions by annealing in the air [14–16]. There are few ways to improve the morphology of thin films. It is changing the annealing atmosphere content (N₂, O₂, Ar) [15]), temperature, and pressure [17].

The fabrication of the lead titanate thin films deposited by reactive magnetron layer-by-layer deposition combined with post-deposition annealing in atmosphere

and vacuum is introduced in this article. The aim of this work was to summarize the results of the solid state reactions between these layers and to investigate the composition, structure and morphology of the PbTiO₃ thin films. The optimal parameters for the dense and flat surface of synthesized lead titanate thin films were obtained.

2. Experiment

The lead titanate oxide thin films were deposited onto silicon (100) substrate by reactive magnetron layer-by-layer deposition at room temperature in O₂ gas environment ($p = 1.33$ Pa). The deposition was realized using substrate periodic parallel to cathodes motion over the magnetrons. The period of motion was 3 s. Pb and Ti disc targets of 3 inch diameter (Kurt J. Lesker Company, Pb and Ti of 99.999% purity) were used during this process. The distance between magnetrons and substrate was kept 65 mm. Deposition rates of each element (PbO₂ and TiO₂) were investigated in order to achieve the desirable stoichiometry for PbTiO₃ phase. The dependence of deposition rates on the plasma discharge current was determined for this purpose. PbO₂ thin films deposition rate dependence on current was linear and about 3–4 times higher than for TiO₂, which is linear, too.

In order to achieve equilibrium of Pb and Ti atoms concentration in thin film, the calculations of molar masses ratio were made for chemical composition of PbTiO₃. According to this, a few PbO₂ and TiO₂ ratios were chosen. TiO₂ deposition rate was a constant at magnetron discharge current $I = 1$ A. The currents of lead cathode were chosen as 0.4, 0.35, and 0.3 A, respectively. The total time of deposition process was 1 h, and the total thickness was chosen and determined as 1 μm. The thickness

*corresponding author; e-mail: aleksandras.iljinas@ktu.lt

was determined using Linnic interferometer and tested with profilometer. The changes of crystallographic composition and surface properties of the structures were investigated after annealing at 670 °C and at 770 °C temperature during one hour in vacuum ($p = 5 \times 10^{-3}$ Pa). The samples were annealed using Tectra Boralectric heating element in vacuum. Few of the samples was annealed at 770 °C temperature during 1 h in conventional furnace in air. The crystalline structure of the samples was investigated by X-ray diffractometer Bruker AXS D8 ADVANCE ($\text{Cu } K_{\alpha}$ radiation, the Bragg–Brentano geometry). The size of film crystallites was determined from the peak broadening by single line and multiple line analysis. Scanning electron microscopy (SEM) surface analysis and energy dispersive spectroscopy (EDS) were investigated using JEOL SM 5600.

3. Results and discussion

The $\text{Pb}/\text{Ti} = 1$ atomic ratio in thin films is necessary in order to achieve good stoichiometry for PbTiO_3 phase. For this purpose the thickness of separate layers was determined from the lead titanate phase formation reaction equation. To achieve atomic ratio $\text{Pb}/\text{Ti} = 1$ the currents of separate cathodes were determined and chosen as $I(\text{Ti}) = 1$ A and $I(\text{Pb}) = 0.4$ A.

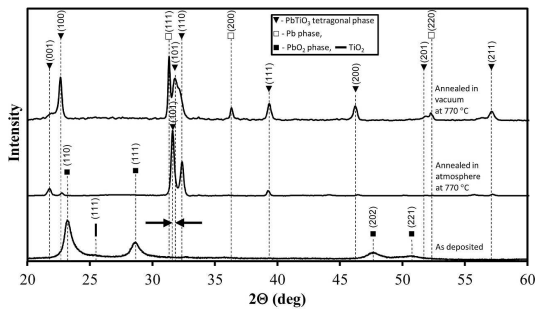


Fig. 1. XRD diagrams of as deposited, annealed in atmosphere and vacuum thin films ($I(\text{Pb}) = 0.4$ A).

Figure 1 shows X-ray diffraction (XRD) diagrams of as deposited and annealed in air atmosphere and vacuum thin films. The mixture of PbO_2 and TiO_2 phases was determined as deposited film. The nanocrystal structure was estimated (average size of crystallites is 14 nm) for PbO_2 and amorphous phase for TiO_2 . Crystallites sizes according to the Thornton model depend on T_s/T_m temperatures ratio, where T_s — substrate temperature and T_m is melting temperature. In our case $T_s/T_m = 0.14$ for TiO_2 , and $T_s/T_m = 0.52$ for PbO_2 . The amorphous phase forms when ratio T_s/T_m is in interval 0.1–0.2. The crystallization process is starting, when ratio is over 0.4.

Annealing in air at 770 °C was chosen to verify the possibility of synthesis tetragonal phase of the perovskite structure from deposited mix of phases. The analysis of the crystal structure was well identified as crystallized tetragonal space group ($P - 4mm$) PbTiO_3

phase [JCPDS-78-299]. Different peaks of the XRD pattern depend on reflections from (001), (100), (101), (111), (110), (200), (201), (220), and (211) planes (Fig. 1, annealed in atmosphere at 770 °C). The results show that pure crystalline phase of 65 nm average size of crystallites was formed. The tetragonality (lattice distortion) $c/a = 1.047$ of thin film is close to the bulk value (1.063) [18].

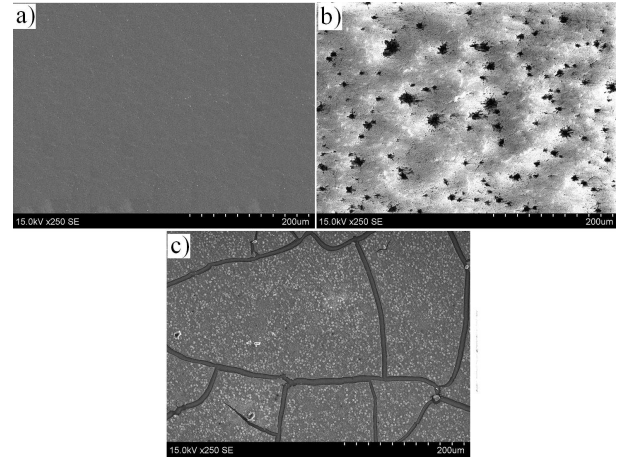


Fig. 2. SEM images of: (a) as deposited, (b) annealed in atmosphere (770 °C), and (c) annealed in vacuum (770 °C) thin films.

Surface morphology is observed by SEM. Surface of deposited, annealed in atmosphere, and annealed in vacuum is shown in Fig. 2. Figure 2a shows that surface of as deposited thin films ($I(\text{Pb}) = 0.4$ A) is uniform and without defects. The morphology of the post-annealed samples is different. The sample after annealing in air atmosphere shows that surface of thin films was very rough and had cracks, holes, and pits (Fig. 2b). The formation of cracks can be explained by high oxidation reaction rate due to oxygen excess, too fast decomposition of PbO_2 to PbO through intermediate phases [19], different reactions initial moments with TiO_2 in different places and high volatility of PbO at higher temperature [17]. Figure 2c shows image of thin films, deposited at the same conditions, but annealed in vacuum (770 °C). Thin film is split to large (of hundred μm) blocks with some distance between them. EDS mapping shows that cracks are through total film thickness, until the Si substrate. This crack indicate that high stress exists in thin film due to lattice mismatch between the film (PbTiO_3) and (Si) substrate on cooling [15].

As it was mentioned above the annealing atmosphere content (N_2 , O_2 [15], Ar [20]) and pressure [17] have impact on the solid state reaction and oxidation rate and therefore the surface morphology. Annealing in vacuum was chosen to slow down the oxidation rate and to form PbTiO_3 tetragonal phase by solid state reactions between mixed (PbO and TiO_2) phases in thin films without influence of oxygen from environment.

The XRD diagrams (Fig. 1, annealed in vacuum at 770 °C) show that thin film has the peaks of PbTiO₃ similar to annealed in air, but broader. That shows that crystallite size is less (39 nm). Two horizontal arrows in Fig. 1 show shifting of (101) peak to higher degrees. It means that lattice is less distorted ($c/a = 1.013$).

Additional peaks which do not belong to lead titanate were identified. The analysis of the crystal structure was well identified as crystallized cubic space group ($Fm\bar{3}m$) of lead phase [JCPDS-4-686]. Different peaks of the XRD pattern belong to reflections from (111), (200), and (220) of pure lead phase. Mix of two phases exists in film. Appearance of pure (not oxide) lead crystallites can be explained due to oxygen deficiency in vacuum and weak chemical covalent of Pb–O bonds [21]. The forming PbTiO₃ phase takes oxygen from lead oxides (PbO₂ or reduced PbO after this decomposition).

The few rates of sputtering of lead cathode (0.4, 0.35, 0.3 A) were chosen in order to investigate the influence of lead amount in films. Thin films were annealed in vacuum after deposition. The XRD results show that lead sputtering rate decrease gives decrease of lead peaks (Fig. 3, $I(\text{Pb}) = 0.35$ A).

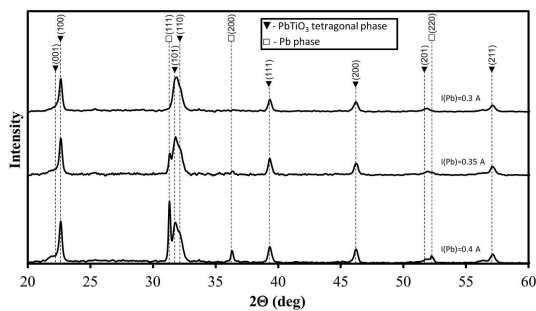


Fig. 3. XRD diagrams of thin films annealed in vacuum at 770 °C.

The decrease of lead sputtering rate (Fig. 3, $I(\text{Pb}) = 0.3$ A) gives pure tetragonal PbTiO₃ phase without lead peaks. These results correlate with EDS measurements of atomic ratio of Pb/Ti in thin films, where Pb/Ti = 1.01, 0.89, 0.80 for $I(\text{Pb}) = 0.4, 0.35, 0.3$ A.

Figure 4 shows SEM images of annealed thin films in vacuum. It is seen that surface structure depends on Pb concentration in thin films. Thin films break with excess of lead (Fig. 2c and Fig. 4a). It breaks to large (few hundred μm) blocks with some distance between them. The distance between blocks is decreasing from $\approx 10 \mu\text{m}$ (Fig. 2c) to $\approx 5 \mu\text{m}$ (Fig. 4a) with decreasing Pb concentration and they disappear at lead and titanium ratio (Pb/Ti = 0.80). Figure 4b shows the unbroken thin film surface. The larger magnification of SEM images shows surface with some ≈ 70 nm pores (Fig. 5).

Thin films breaks can be explained by different specific volumes of Pb ($8.8 \times 10^{-5} \text{ m}^3/\text{kg}$) and PbTiO₃ ($13.3 \times 10^{-5} \text{ m}^3/\text{kg}$). The volume of mixed phases (Pb and PbTiO₃) is smaller than of pure lead titanate phase

after solid state reactions in thin films due to lead excess. Therefore the material shrinks. No shrinking appears when lead concentration in thin film is less. Therefore, the best results at Pb/Ti = 0.80 or $I(\text{Pb}) = 0.3$ A were obtained. It contradicts our supposition that atomic ratio should be Pb/Ti = 1. It explains that reaction processes of PbTiO₃ phase formation in atmosphere are going differently than processes using annealing in vacuum.

Annealing in vacuum at 670 °C was performed in order to investigate the formation of PbTiO₃ phase at lower temperatures.

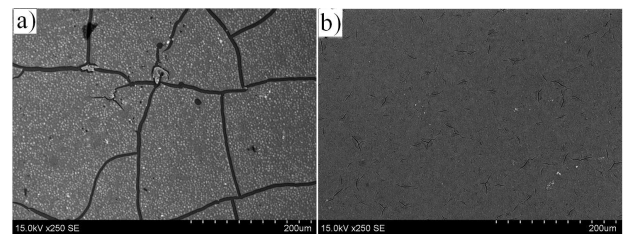


Fig. 4. SEM images of as deposited and annealed in vacuum at 770 °C temperature PbTiO₃ thin films a) $I(\text{Pb}) = 0.35$ A, b) $I(\text{Pb}) = 0.3$ A.

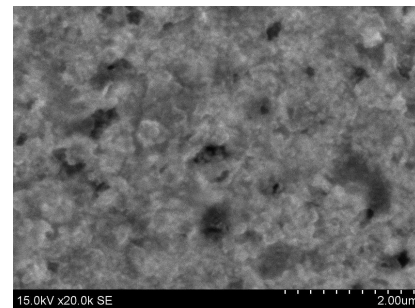


Fig. 5. SEM images of annealed in vacuum at 770 °C PbTiO₃ thin films $I(\text{Pb}) = 0.3$ A.

The XRD results showed the formation of pseudocubic PbTiO₃ phase at 670 °C annealing temperature. No lattice distortion was observed. This structure does not exhibit ferroelectric properties [22, 23].

4. Conclusions

Perovskite PbTiO₃ nanostructure thin films were synthesized by using reactive magnetron layer-by-layer deposition and post annealing in air, and vacuum on silicon substrate. The structure and morphology of thin films strongly depends on annealing environment. Tetragonal PbTiO₃ phase (with tetragonality $c/a = 1.047$ and crystallinity ≈ 64 nm) was formed by annealing thin films in air (770 °C), but surface of these films was very rough and had cracks. The structure of post annealed thin films in vacuum depends on Pb/Ti atomic ratio. The best structure (without breaks) was formed when atomic ratio was

Pb/Ti = 0.80. Crystallinity and the lattice tetragonality for these structures was lower than structures annealed in air. Vacuum annealing improves PbTiO₃ thin film formability through the reduction in internal stresses and improved microstructural characteristics.

Acknowledgments

This research was funded by a grant (No. MIP-069/2013) from the Research Council of Lithuania.

References

- [1] G. Shirane, S. Hoshino, K. Suzuki, *Phys. Rev.* **80**, 1105 (1950).
- [2] H. Zhao, J. Wang, C. Sun, J. Chen, A. Ablat, E. Muhammed, K. Ibrahim, S. Qiao, L. Qiao, X. Xing, *Thin Solid Films* **542**, 155 (2013).
- [3] L. Fan, J. Chen, Q. Wang, J. Deng, R. Yu, X. Xing, *Ceram. Int.* **40**, 7723 (2014).
- [4] D. Szwagierczak, J. Kulawik, *J. Eur. Ceram. Soc.* **24**, 1979 (2004).
- [5] S. Cochran, in: *Ultrasonic Transducers*, Ed. K. Nakamura, Woodhead Publ., Oxford U.K. 2012, p. 3.
- [6] J. Zhao, L. Li, Z. Gui, *Mater. Sci. Eng. B* **94**, 202 (2002).
- [7] L.L. Sun, O.K. Tan, W.G. Liu, W.G. Zhu, X. Yao, *Infrared Phys. Technol.* **44**, 177 (2003).
- [8] B. Fang, K. Qian, N. Yuan, J. Ding, X. Zhao, H. Luo, *Mater. Lett.* **84**, 91 (2012).
- [9] F. Bensebaa, in: *Interface Science and Technology*, Ed. B. Farid, Elsevier, 2013, Ch. 7, p. 429.
- [10] K. Kim, Y.J. Song, *Microelectron. Reliab.* **43**, 385 (2003).
- [11] H. Takasu, *Microelectron. Eng.* **59**, 237 (2001).
- [12] B. Li, X. Zhang, J.B. Wang, X.L. Zhong, F. Wang, Y.C. Zhou, *Mech. Res. Commun.* **55**, 40 (2014).
- [13] N.A. Basit, H.K. Kim, J. Blachere, *Thin Solid Films* **302**, 155 (1997).
- [14] F.M. Pontes, J.H.G. Rangel, E.R. Leite, E. Longo, J.A. Varela, E.B. Araujo, J.A. Eiras, *Thin Solid Films* **366**, 232 (2000).
- [15] J. Harjuoja, A. Kosola, M. Putkonen, N. Niinisto, *Thin Solid Films* **496**, 346 (2006).
- [16] V. Stankus, J. Dudonis, *Mater. Sci. Eng. B* **109**, 178 (2004).
- [17] R. Thapliyal, P. Schwaller, M. Amberg, F.J. Haug, G. Fortunato, D. Hegemann, H.J. Hug, A. Fischer, *Surf. Coat. Technol.* **200**, 1051 (2005).
- [18] F. Jona, G. Shirane, *Ferroelectric Crystals*, Dover Publ., New York 1993 p. 402.
- [19] W.-B. Cai, Y.-Q. Wan, H.-T. Liu, W.-F. Zhou, *J. Electroanal. Chem.* **387**, 95 (1995).
- [20] Q. Zhao, Z.X. Fan, Z.S. Tang, X.J. Meng, J.L. Song, G.S. Wang, J.H. Chu, *Surf. Coat. Technol.* **160**, 173 (2002).
- [21] S. de Lazaro, E. Longo, J.R. Sambrano, A. Beltran, *Surf. Sci.* **552**, 149 (2004).
- [22] S. Wongsanmai, X. Tan, S. Ananta, R. Yimnirum, *J. Alloys Comp.* **454**, 331 (2008).
- [23] G. Yu, X. Dong, G. Wang, F. Cao, X. Chen, *J. Alloys Comp.* **500**, 56 (2010).